Letter

Interaction quenches in nonzero-temperature fermionic condensates

H. Kurkjian [1,2,*] V. E. Colussi [3,4] P. Dyke [5] C. Vale [5] and S. Musolino [6]
[1] *Laboratoire de Physique Théorique de la Matière Condensée, Sorbonne Université, CNRS, 75005, Paris, France*
[2] *Laboratoire de Physique Théorique, Université de Toulouse, CNRS, UPS, 31400, Toulouse, France*
[3] *Infleqtion, Inc., 3030 Sterling Circle, Boulder, Colorado 80301, USA*
[4] *Pitaevskii BEC Center, CNR-INO and Dipartimento di Fisica, Università di Trento, 38123 Trento, Italy*
[5] *Optical Sciences Centre, ARC Centre of Excellence in Future Low-Energy Electronics Technologies, Swinburne University of Technology, Melbourne 3122, Australia*
[6] *Université Côte d'Azur, CNRS, Institut de Physique de Nice, 06200 Nice, France*

(Received 11 October 2023; revised 14 March 2024; accepted 22 March 2024; published 29 April 2024)

We revisit the study of amplitude oscillations in a pair condensate of fermions after an interaction quench, and generalize it to nonzero temperature. For small variations of the order parameter, we show that the energy transfer during the quench determines both the asymptotic pseudoequilibrated value of the order parameter and the magnitude of the oscillations, after multiplication by, respectively, the static response of the order parameter and spectral weight of the pair-breaking threshold. Since the energy transferred to the condensed pairs decreases with temperature as the superfluid contact, the oscillations eventually disappear at the critical temperature. For deeper quenches, we generalize the regimes of persistent oscillations and monotonic decay to nonzero temperatures, and explain how they become more abrupt and are more easily entered at high temperatures when the ratio of the initial to final gap either diverges, when quenching toward the normal phase, or tends to zero, when quenching toward the superfluid phase. Our results are directly relevant for existing and future experiments on the nonequilibrium evolution of Fermi superfluids near the phase transition.

DOI: 10.1103/PhysRevA.109.L041302

Introduction. Fermionic condensates, unlike most of their bosonic counterparts, are made of composite objects, known as Cooper pairs. This internal structure implies more degrees of freedom beyond the usual sound waves found in bosonic systems [1]. At the individual level, single Cooper pairs can break into two unpaired fermions, which leads to a gapped spectrum of fermionic quasiparticles [2]. At the many-body level, whole wave packets of quasiparticles can be excited, for example, by tuning the interparticle interaction strength [3]. This causes the amplitude of the order parameter to oscillate in a characteristic way [4], with a frequency and damping determined by the spectral distribution of the wave packet.

In contrast with the typical picture of amplitude or Higgs modes relying on a single complex bosonic field [5] in a Mexican hat potential, amplitude oscillations in a fermionic condensate are an intrinsically many-body effect, emerging only from the superposition of individual quasiparticle vibrations [4,6–8]. Still, for spatially dependent and weak perturbations of the interaction strength, the evolution of the excited quasiparticle wave packet can be summarized by a single pole of the order-parameter response function, such that the oscillations can be interpreted as a damped collective mode [9,10].

The case of homogeneous (zero-momentum) perturbations is more subtle: one can no longer identify a pole in the order-parameter response function, such that the collective mode disappears. There remains, however, a non-Lorentzian singularity in the spectral function, right at the threshold energy for breaking Cooper pairs. In the time domain, this converts into the famous power-law decaying oscillations of the order parameter [4]. The density of quasiparticle states available around the pair-breaking threshold changes depending on whether the gapped fermionic spectrum has its minimum at zero or nonzero momentum, corresponding, respectively, to the Bose-Einstein condensate (BEC) or Bardeen-Cooper-Schrieffer (BCS) regimes. The lower density of states in the BEC regime makes the damping exponent increase to $3/2$, compared to $1/2$ in the BCS regime [7].

This remarkable collective effect has recently been the center of much experimental attention with ultracold fermionic atoms [11,12], superconductors [13], and cavity QED simulators [14,15]. The observations in those experiments have revealed some important limits in our theoretical understanding of the oscillations. Previous studies [7,8] have been restricted to zero temperature, whereas experimentally the oscillations have been recorded from low temperature to the vicinity of the phase transition. Additionally, important observables [12], such as the magnitude of the oscillations or the asymptotic limit of the order parameter, have not yet been fully understood.

Here, we show that oscillations of the order parameter for small interaction quenches in the regime of linear response have the same form at zero and nonzero temperature: the power-law damping retains the same exponent, and the oscillation frequency 2Δ simply decreases with temperature as the gap Δ. However, the presence of thermally excited quasiparticles before the quench limits the variation of the order parameter, which, in contrast to the zero-temperature case, no

*Corresponding author: hadrien.kurkjian@cnrs.fr

longer tends at long time to its value expected following an adiabatic change of the interaction strength. We interpret the magnitude of the oscillations as the product of the spectral weight of the pair-breaking threshold with the energy change during the quench, itself related to the change in the scattering length through the contact.

We also argue that nonlinear effects increase near the critical temperature since the ratio of the initial to final equilibrium gap Δ_i/Δ_f either diverges or tends to zero when the depth of the interaction quench is kept fixed. The regime of power-law damped oscillations is thus hidden by the nonlinear regimes of persistent oscillations (regime III of Ref. [8]) or overdamped evolution (regime I), and the evolution in those two regimes becomes more abrupt compared to low temperatures.

Model. We consider a balanced two-component Fermi gas trapped in a three-dimensional volume V at temperature $T = 1/\beta$ (we use $\hbar = k_B = 1$ throughout this Letter), with contact interactions between $\uparrow$ and $\downarrow$ components. The density ρ of the gas fixes the Fermi wave number $k_F = (3\pi^2\rho)^{1/3}$, and the bare coupling constant g is renormalized [16] to yield the appropriate s-wave scattering length a. In the mean-field approximation, the homogeneous system evolves according to the time-dependent BCS equations [17]

$$i\partial_t c_{\mathbf{k}} = (k^2/m)c_{\mathbf{k}} + \Delta(1 - 2n_{\mathbf{k}}), \quad (1)$$

$$i\partial_t n_{\mathbf{k}} = \Delta c_{\mathbf{k}}^* - \Delta^* c_{\mathbf{k}}, \quad (2)$$

where m is the atomic mass, $n_{\mathbf{k}} = \langle \hat{a}_{\mathbf{k}\uparrow}^\dagger \hat{a}_{\mathbf{k}\uparrow}\rangle = \langle \hat{a}_{\mathbf{k}\downarrow}^\dagger \hat{a}_{\mathbf{k}\downarrow}\rangle$ the momentum distribution, $c_{\mathbf{k}} = \langle \hat{a}_{-\mathbf{k}\downarrow}\hat{a}_{\mathbf{k}\uparrow}\rangle$ the pairing wave function, and $\Delta = g\int d^3k\, c_{\mathbf{k}}/(2\pi)^3$ the order parameter.

Before the quench, the gas is at equilibrium at temperature T_i, chemical potential μ_i, and scattering length a_i. This corresponds to the static solution of the BCS equations, that is, the usual BCS thermal state with $n_{\mathbf{k},i} = \{1 - [1 - 2F(\epsilon_{\mathbf{k}})]\xi_{\mathbf{k}}/\epsilon_{\mathbf{k}}\}/2$ and $c_{\mathbf{k},i} = -[1 - 2F(\epsilon_{\mathbf{k}})]\Delta_i/2\epsilon_{\mathbf{k}}$, in terms of the free-fermion and BCS dispersion relations, $\xi_{\mathbf{k}} = k^2/2m - \mu_i$ and $\epsilon_{\mathbf{k}} = \sqrt{\xi_{\mathbf{k}}^2 + \Delta_i^2}$, and Fermi-Dirac distribution $F(\epsilon) = 1/(1 + e^{\epsilon/T_i})$. The abrupt variation of a from a_i to a_f leaves the microscopic variables unchanged [$n_{\mathbf{k}}(t = 0^+) = n_{\mathbf{k},i}$ and similarly for $c_{\mathbf{k}}$] but affects the coupling constant through

$$\frac{1}{g_f} - \frac{1}{g_i} = \left(\frac{1}{a_f} - \frac{1}{a_i}\right)\frac{m}{4\pi}, \quad (3)$$

obtained via the Lippmann-Schwinger equation [18,19].

The initial kink in the order parameter then follows from the gap equation

$$\Delta(t = 0^+) - \Delta_i = \frac{g_f - g_i}{g_i}\Delta_i. \quad (4)$$

This kink corresponds to an energy variation that is proportional to the volumic contact C [20–25]:

$$\epsilon \equiv \frac{E_f - E_i}{V} = -\frac{C}{4\pi m}\left(\frac{1}{a_f} - \frac{1}{a_i}\right). \quad (5)$$

While Eq. (5) is valid in general, the BCS approximation of the contact is $C_{\mathrm{BCS}} = m^2\Delta^2$. This expression vanishes at the critical temperature as BCS theory approximates the normal phase by an ideal gas, and restricts the contact to the contribution of the condensed pairs. For the general description of the gas, this is a rather crude approximation, in particular, near the critical temperature, but for the amplitude oscillations studied in this Letter, the superfluid contact is precisely the important quantity.[1]

Linear response. Shallow quenches are generally characterized by a small injected energy per particle, although this rule is brought into question later in this Letter. In this weakly excited regime, one can linearize the BCS system Eqs. (1) and (2) around the initial equilibrium state and solve using the Laplace transformation [7,26] (see Appendix A). With the initial condition (4), the phase of the order parameter is not excited, and only its modulus evolves as

$$\Delta(t) = \Delta_\infty - \epsilon\int_{\omega_{\mathrm{th}}}^{+\infty}\frac{2d\omega}{\pi}\frac{\cos\omega t}{\omega}\mathrm{Im} f(\omega + i0^+). \quad (6)$$

This expression is composed of an asymptotic value Δ_∞ reached when $t \to +\infty$, and a time-dependent, oscillatory part, written as the frequency integral of the order-parameter modulus-modulus response function

$$f(z) = -\frac{M_{11}(z)}{\Delta_i\left[M_{11}(z)M_{22}(z) - M_{12}^2(z)\right]} \quad (7)$$

over the pair-breaking continuum, bounded only from below by the threshold ω_{th}. The linear response matrix M_{ij} appearing here is given by integrals over the internal degrees of freedom of the Cooper pairs $M_{11}/z^2 = M_{22}/(z^2 - 4\Delta_i^2) = \int \frac{d^3k}{(2\pi)^3}\frac{1-2F(\epsilon_{\mathbf{k}})}{2\epsilon_{\mathbf{k}}(z^2-4\epsilon_{\mathbf{k}}^2)}$ and $M_{12} = M_{21} = \int \frac{d^3k}{(2\pi)^3}\frac{z\xi_{\mathbf{k}}[1-2F(\epsilon_{\mathbf{k}})]}{\epsilon_{\mathbf{k}}(z^2-4\epsilon_{\mathbf{k}}^2)}$.

Quite intuitively, the final shift in Δ, obtained when the oscillations have decayed, is the product of the transferred energy and static modulus response $f(\omega = 0)$:

$$\Delta_\infty = \Delta_i + f(0)\epsilon. \quad (8)$$

We identify here an important effect of temperature on the postquench dynamics. When $T_i = 0$, the asymptotic gap Δ_∞ matches the equilibrium gap Δ_f that would be reached after an adiabatic change of the scattering length from a_i to a_f. This is due to the static modulus response saturating the injected energy $f(0) = d\Delta/d\epsilon$. This is no longer true for $T_i > 0$, and instead

$$|\Delta_\infty - \Delta_i| < |\Delta_f - \Delta_i|. \quad (9)$$

In other words, the order parameter remains closer to its initial value than it would under an adiabatic transformation, as a part of the injected energy is absorbed by the thermally excited quasiparticles. In the limit $T \to T_c$, the ratio $(\Delta_\infty - \Delta_i)/(\Delta_f - \Delta_i)$ (shown in Fig. 1) vanishes as $\Delta(T)$ in the BCS regime ($\mu > 0$) and as $\Delta^2(T)$ in the BEC regime. In the BCS limit ($1/k_F a \to -\infty$), where time-dependent BCS theory is most reliable, we extracted the limiting behavior (for

[1]While the inverse coupling constants $1/g_i$ and $1/g_f$ diverge linearly with a momentum cutoff, their difference does not, according to Eq. (3). Thus, the injected energy [Eq. (5)] remains finite and nonzero, while the discontinuity in Δ [Eq. (4)] vanishes. This is a consequence of the formally divergent interaction energy $E_{\mathrm{int}} = \Delta^2/g$ according to BCS theory.

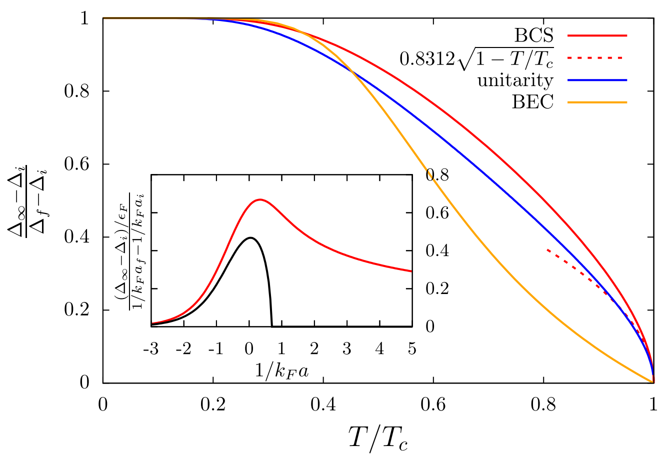

FIG. 1. The asymptotic change of the order parameter $\Delta_\infty - \Delta_i$ measured relative to the change $\Delta_f - \Delta_i$ under an adiabatic evolution, as a function of temperature at unitarity, in the BCS and BEC limits. At $T = 0$, $\Delta_\infty = \Delta_f$ despite the nonadiabatic nature of the quench. Near T_c, we indicate the asymptotic behavior in the BCS limit, Eq. (10). (Inset) The change $\Delta_\infty - \Delta_i$ (in units of ϵ_F) relative to the change in the scattering length $1/k_F a_f - 1/k_F a_i$ throughout the BEC-BCS crossover at $T = 0$ (red curve) and $T \to T_c$ (black curve). In both cases, a maximum is reached near unitarity. Note that the change remains nonzero (in units of ϵ_F) on the BCS side ($\mu > 0$), which means the linear approximation breaks down (if the quench depth $1/k_F a_f - 1/k_F a_i$ is kept independent of temperature).

details, see Ref. [27] and the Supplemental Material [28]):

$$\frac{\Delta_\infty - \Delta_i}{\Delta_f - \Delta_i} \underset{\substack{1/k_F a \to -\infty \\ T \to T_c}}{\simeq} 0.8312\sqrt{1 - T/T_c}. \tag{10}$$

Note that at both zero and nonzero initial temperature, the state reached asymptotically is not an equilibrium state and, in particular, does not have a well-defined temperature. To describe equilibration, the integrable BCS system should be replaced by an ergodic model.

Equation (8) provides a criterion for the validity of the linear regime. For the deviation of the order parameter to remain small, it is necessary and sufficient that $|\Delta_\infty - \Delta_i| \ll \Delta_i$. At low temperatures, Δ_i is comparable to the Fermi energy ϵ_F, so this condition simply translates into $|a_f - a_i| \ll a_i$, which is not a particularly demanding constraint. Near T_c, however, $(\Delta_\infty - \Delta_i)/(1/k_F a_f - 1/k_F a_i)$ is comparable to ϵ_F (as shown by the black curve in Fig. 1) and hence much larger than Δ_i, which scales as $\sqrt{T_c - T_i}$. This leads to a stricter condition $|a_f - a_i| \ll a_i \Delta_i/\epsilon_F$ for the validity of the linear approximation. In other words, the quench depth $|1 - a_i/a_f|$ has to be scaled as $\Delta_i/\epsilon_F \approx \sqrt{1 - T_i/T_c}$ in order for the time evolution of Δ to remain in the linear regime. This explains why the linear approximation is always violated for T_i sufficiently close to T_c in an experimental scenario such as Ref. [12], where the quench depth is fixed independently of temperature.

We now turn to the time evolution described by Eq. (6). The continuity of $\Delta(t)$ at $t = 0$ is guaranteed by the sum rule of the modulus-modulus response function: $\int_{+\infty+i0^+}^{-\infty+i0^+} dz f(z)/2i\pi z = 0$. Then, at long times, the nature of the oscillations of $\Delta(t)$ depends on the behavior of f in the vicinity of the pair-breaking threshold $\omega_{\rm th}$. In the BCS regime ($\mu_i > 0$) and irrespective of the temperature, the response function has a square root divergence near $\omega_{\rm th} = 2\Delta_i$. Conversely, in the BEC regime ($\mu_i < 0$) at all temperatures, the response function is canceled as a square root near the dimer-breaking threshold:

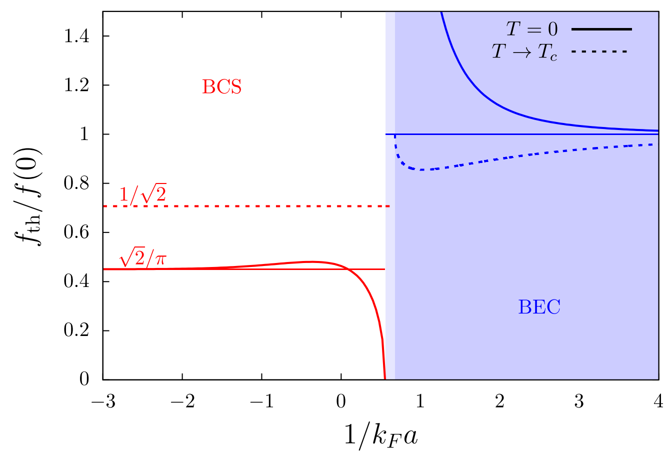

FIG. 2. The spectral weight of the pair-breaking edge $f_{\rm th}$ [relative to the static response $f(0)$] as a function of the interaction strength at $T = 0$ (solid curves) and $T \to T_c$ (dashed curves). In red is the BCS regime where the edge exhibits a square root divergence [upper line of Eq. (11)], and in blue is the BEC regime where instead this edge is a square root cancellation [lower line of Eq. (11)]. Note that the boundary between those two regimes (shaded area) shifts from $1/k_F a \simeq 0.55$ at $T = 0$ to $1/k_F a \simeq 0.68$ at $T \to T_c$.

$$\mathrm{Im} f(\omega + i0^+) \underset{\omega\to\omega_{\rm th}}{\sim} \begin{cases} f_{\rm th}\sqrt{\frac{\omega_{\rm th}}{\omega-\omega_{\rm th}}} \text{ when } \mu_i > 0 \\ f_{\rm th}\sqrt{\frac{\omega-\omega_{\rm th}}{\omega_{\rm th}}} \text{ when } \mu_i < 0 \end{cases}. \tag{11}$$

After the frequency integration, these behaviours near $\omega_{\rm th}$ translate into power-law attenuated oscillations of $\Delta(t)$:

$$\frac{\Delta(t) - \Delta_\infty}{\Delta_i - \Delta_\infty} \underset{t\to+\infty}{\sim} \begin{cases} \frac{f_{\rm th}}{f(0)}\sqrt{\frac{4}{\pi\omega_{\rm th}t}}\cos\left(\omega_{\rm th}t + \frac{\pi}{4}\right), \mu_i > 0 \\ \frac{f_{\rm th}}{f(0)}\frac{1}{\sqrt{\pi\omega_{\rm th}^3 t^3}}\cos\left(\omega_{\rm th}t + \frac{3\pi}{4}\right), \mu_i < 0 \end{cases}. \tag{12}$$

The spectral weight $f_{\rm th}$ which characterizes the asymptotic behaviors at the threshold is shown in Fig. 2 as a function of the interaction regime. Comparing the zero-temperature case (solid curves) to the vicinity of T_c (dashed curves), we observe a suppression of the relative weight $f_{\rm th}/f(0)$ on the BEC side but an increase on the BCS side. While this increase *a priori* favors the observability of the power-law damped oscillations, we note that $f_{\rm th}/f(0)$ characterizes the amplitude of the signal only when scaled to the asymptotic change in Δ, see Eq. (12). Scaled to the adiabatic variation $\Delta_f - \Delta_i$, the amplitude will vanish as $\Delta_\infty - \Delta_i$ as shown by Fig. 1.

Quenches in the nonlinear regime. The fact that the nonlinearity increases with temperature (as long as the quench depth $|a_i - a_f|$ is fixed) suggests extending our study to the nonlinear regime. We do this numerically by simulating Eqs. (1) and (2) on a fine momentum grid.

We recall the zero-temperature quench diagram of Ref. [8] (see Fig. 5 therein) that identified three qualitatively dis-

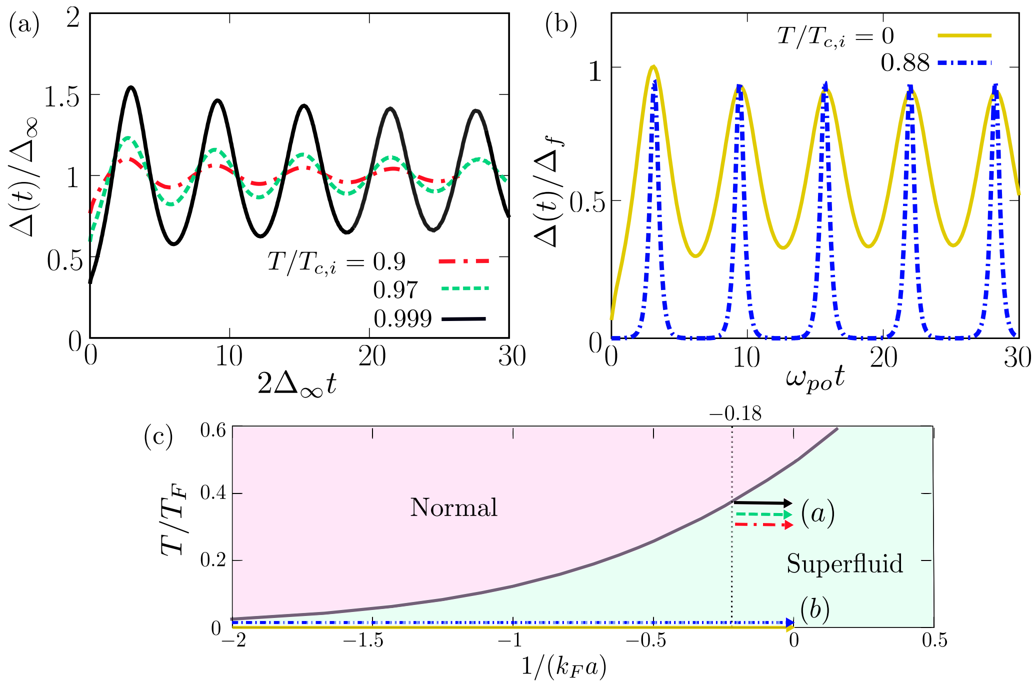

FIG. 3. (a) The onset of regime III (persistent oscillations) in a quench from $1/(k_F a_i) = -0.18$ to $1/(k_F a_f) = 0$ when raising the initial temperature. (b) Effect of temperature on the persistent oscillations for a quench from $1/(k_F a_i) = -2$ to $1/(k_F a_f) = 0$ belonging to regime III at all temperatures. To make the curves oscillate in phase, we introduce here the frequency $\omega_{po} = 0.6(2\Delta_f)$ at zero temperature and $0.13(2\Delta_f)$ at $T = 0.88T_{c,i}$. (c) Illustration of the quenches studied in (a) and (b) in the $[1/(k_F a), T/T_F]$ plot.

tinct regimes in the (Δ_i, Δ_f) plane. In regime I, there are no oscillations as $\Delta(t)$ is overdamped; this regime includes, in particular, the limit $\Delta_i \gg \Delta_f$. Regime II is the regime of power-law damped oscillations, which contains the linear regime on the diagonal $\Delta_i \simeq \Delta_f$. Finally, a regime III of undamped oscillations was identified around the limit $\Delta_f \gg \Delta_i$.

We show now how regimes I and III generalize to nonzero temperatures and tend to hide regime II when the initial state approaches the critical point ($T_i \to T_{c,i}$) and the quench depth is fixed. For an initial state in the regime $|T - T_c| \ll T_c$, that is, $\Delta_i \ll \epsilon_F$, quenches in the direction of the superfluid phase end up in $\Delta_f \approx \epsilon_F \gg \Delta_i$, and therefore in regime III of persistent oscillations. Conversely, quenches toward the normal phase yield $\Delta_i \gg \Delta_f = 0$, and thus fall into the overdamped regime I.

In Fig. 3, we illustrate the onset of regime III at high temperatures when quenching in the direction of the superfluid phase. Going from the BCS side ($a_i < 0$) to unitarity, with a quench depth sufficiently low to be in regime II at $T = 0$, as in Fig. 3(a), we notice an increase of the oscillation amplitude (scaled to Δ_∞), which precedes the appearance of persistent oscillations at temperatures close to $T_{c,i}$. The persistent oscillations also become much more abrupt than at low temperature, as illustrated by Fig. 3(b), where the quench depth is chosen to be in regime III already at $T = 0$.

In Fig. 4, we consider the opposite case of quenches toward the normal phase with $1/a_i = 0$ and a_f on the BCS side. As shown in Fig. 4(a), quenches sufficiently shallow to be in regime II at low temperatures undergo a gradual decrease of their asymptotic limit and oscillation frequency (both determined by Δ_∞) with temperature, up to a point where the order parameter tends to zero and no longer oscillates. In Fig. 4(a), this occurs at $T/T_c = 0.999$, corresponding to $\Delta_f/\Delta_i \sim 2 \times 10^{-4}$. This threshold of regime I is reached at a lower temperature for larger quench depths. When the quench is sufficiently deep to be in regime I already at $T = 0$, it remains in this regime at all temperatures, and the decay of $\Delta(t)$ becomes more abrupt, as illustrated by Fig. 4(b).

Conclusion. We have studied amplitude oscillations in a nonzero temperature fermionic condensate within time-dependent BCS theory. We showed how the magnitude of the oscillations and the asymptotic change of the order parameter $\Delta_\infty - \Delta_i$ are both proportional to the BCS contact. The oscillations thus fade out as this contact vanishes at the phase transition. While the oscillation frequency is predicted to vanish at T_c as Δ on the BCS side, it stays nonzero on the BEC side and coincides with the molecular binding energy $E_{\rm mol} = 2|\mu|$. The fact that time-dependent BCS theory does not correctly describe the normal phase of the interacting gas limits our description of what happens outside the superfluid phase in particular during dynamical phase transitions [29]. Going beyond BCS theory, one can also imagine that amplitude oscillations would occur in the pseudogap regime at (twice) the pseudogap frequency, rather than at the BCS gap frequency; amplitude oscillations could therefore persist in the normal phase [30,31].

Acknowledgments. We thank Denise Ahmed-Braun and Servaas Kokkelmans for valuable discussions. V.E.C. acknowledges financial support from the Provincia Autonoma di Trento, the Italian MIUR under the PRIN2017 project-CEnTraL and the National Science Foundation under Grant

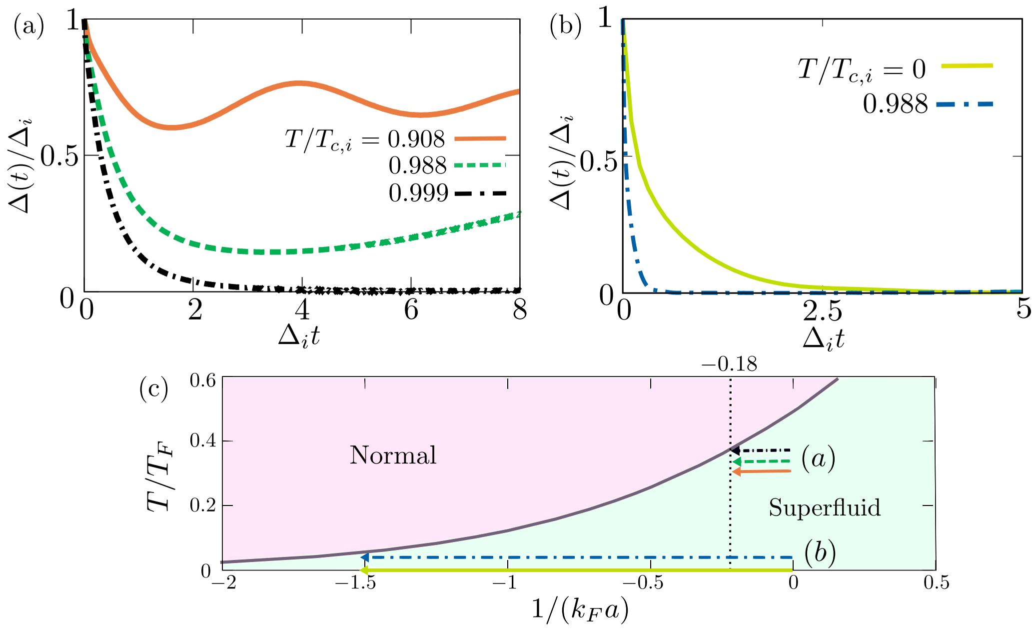

FIG. 4. (a) The onset of regime I (overdamped evolution) when raising the initial temperature of quenches from $1/(k_F a_i) = 0$ to $1/(k_F a_f) = -0.18$. (b) The decay of $\Delta(t)$ becomes more abrupt at higher temperature, as shown here for a quench from $1/(k_F a_i) = 0$ to $1/(k_F a_f) = -1.5$ belonging to regime I at all temperatures. (c) Illustration of the quenches studied in (a) and (b) in the $[1/(k_F a), T/T_F]$ plot.

No. NSF PHY-1748958. S.M. acknowledges financial support from the ANR-21-CE47-0009 Quantum-SOPHA project.

Appendix A: Linearization of the Hartree-Fock-Bogoliubov equations. We give here additional details on our analytical solution of the BCS equations (1) and (2) in the regime of weak perturbations, leading to Eq. (6). We linearize the evolution around the initial equilibrium state, rather than around a virtual final equilibrium state as in Ref. [7]. At nonzero temperature, where $\Delta(t)$ never reaches Δ_f, this is far more intuitive.

We introduce the fluctuations $\delta c_{\mathbf{k}} = c_{\mathbf{k}} - c_{\mathbf{k},i}$, $\delta n_{\mathbf{k}} = n_{\mathbf{k}} - n_{\mathbf{k},i}$, and $\delta\Delta = \Delta - \Delta_i$ and linearize the BCS system (1) and (2):

$$\mathrm{i}\partial_t \delta c_{\mathbf{k}} = 2\xi_{\mathbf{k}}\delta c_{\mathbf{k}} - 2\Delta_i \delta n_{\mathbf{k}} + \frac{\xi_{\mathbf{k}}}{\epsilon_{\mathbf{k}}} F(\epsilon_{\mathbf{k}})\delta\Delta \tag{A1}$$

$$\mathrm{i}\partial_t \delta n_{\mathbf{k}} = -\Delta_i(\delta c_{\mathbf{k}} - \delta c_{\mathbf{k}}^*) - \frac{\Delta_i}{2\epsilon_{\mathbf{k}}} F(\epsilon_{\mathbf{k}})(\delta\Delta - \delta\Delta^*). \tag{A2}$$

Although the quench scenario corresponds to $\delta n_{\mathbf{k}} = \delta c_{\mathbf{k}} = 0$ at $t = 0^-$, we make so far no assumption on the initial state. In this more general case, the fluctuation of Δ has a time-dependent part caused by the δc, and a constant part $\delta\Delta_0 = \frac{g_f - g_i}{V} \sum_{\mathbf{k}} c_{\mathbf{k},i}$ caused by the quench on g:

$$\delta\Delta(t) = \frac{g_i}{V} \sum_{\mathbf{k}} \delta c_{\mathbf{k}}(t) + \delta\Delta_0. \tag{A3}$$

In the spirit of Ref. [32], we now move to the quasiparticle basis

$$\alpha_{\mathbf{k}}^+ = \frac{\xi_{\mathbf{k}}}{\epsilon_{\mathbf{k}}}(\delta c_{\mathbf{k}} + \delta c_{\mathbf{k}}^*) - \frac{2\Delta_i}{\epsilon_{\mathbf{k}}}\delta n_{\mathbf{k}}$$

$$\alpha_{\mathbf{k}}^- = \delta c_{\mathbf{k}} - \delta c_{\mathbf{k}}^* \tag{A4}$$

$$m_{\mathbf{k}} = \frac{2\xi_{\mathbf{k}}}{\epsilon_{\mathbf{k}}}\delta n_{\mathbf{k}} + \frac{\Delta_i}{\epsilon_{\mathbf{k}}}(\delta c_{\mathbf{k}} + \delta c_{\mathbf{k}}^*) \tag{A5}$$

so as to diagonalize the individual parts of Eqs. (A1) and (A2):

$$\mathrm{i}\partial_t \alpha_{\mathbf{k}}^+ = 2\epsilon_{\mathbf{k}}\alpha_{\mathbf{k}}^- + F(\epsilon_{\mathbf{k}})(\delta\Delta - \delta\Delta^*) \tag{A6}$$

$$\mathrm{i}\partial_t \alpha_{\mathbf{k}}^- = 2\epsilon_{\mathbf{k}}\alpha_{\mathbf{k}}^+ + \frac{\xi_{\mathbf{k}}}{\epsilon_{\mathbf{k}}} F(\epsilon_{\mathbf{k}})(\delta\Delta + \delta\Delta^*) \tag{A7}$$

$$\mathrm{i}\partial_t m_{\mathbf{k}} = 0. \tag{A8}$$

In the quasiparticle basis, the fluctuations of Δ take the form

$$\delta\Delta = \delta\Delta_0 + \frac{g_i}{2} \int \frac{\mathrm{d}^3 k}{(2\pi)^3} \left[\alpha_{\mathbf{k}}^- + \frac{\xi_{\mathbf{k}}}{\epsilon_{\mathbf{k}}}\alpha_{\mathbf{k}}^+ + \frac{\Delta_i}{\epsilon_{\mathbf{k}}} m_{\mathbf{k}}\right]. \tag{A9}$$

To solve the time-dependent system, we introduce the Laplace transform of the variables

$$A_{\mathbf{k}}^\pm(\omega) = \int_{0^-}^{+\infty} \mathrm{e}^{\mathrm{i}\omega t} \alpha_{\mathbf{k}}^\pm(t)\mathrm{d}t, \tag{A10}$$

and similarly, for $M_{\mathbf{k}}(\omega)$ and $\delta_\pm(\omega)$, the transform of $m_{\mathbf{k}}(t)$ and $\delta\Delta(t) \pm \delta\Delta^*(t)$, respectively. This allows us to express the microscopic variables in terms of the fluctuations of Δ,

$$A_{\mathbf{k}}^+(\omega) = \frac{\mathrm{i}\omega\alpha_{\mathbf{k}}^+(0^-) + 2\mathrm{i}\epsilon_{\mathbf{k}}\alpha_{\mathbf{k}}^-(0^-)}{\omega^2 - 4\epsilon_{\mathbf{k}}^2} + \frac{2\xi_{\mathbf{k}} F(\epsilon_{\mathbf{k}})}{\omega^2 - 4\epsilon_{\mathbf{k}}^2}\delta_+(\omega)$$
$$+ \frac{\omega F(\epsilon_{\mathbf{k}})}{\omega^2 - 4\epsilon_{\mathbf{k}}^2}\delta_-(\omega) \tag{A11}$$

$$A_{\mathbf{k}}^-(\omega) = \frac{\mathrm{i}\omega\alpha_{\mathbf{k}}^-(0^-) + 2\mathrm{i}\epsilon_{\mathbf{k}}\alpha_{\mathbf{k}}^+(0^-)}{\omega^2 - 4\epsilon_{\mathbf{k}}^2} + \frac{2\epsilon_{\mathbf{k}} F(\epsilon_{\mathbf{k}})}{\omega^2 - 4\epsilon_{\mathbf{k}}^2}\delta_-(\omega)$$
$$+ \frac{\omega\xi_{\mathbf{k}} F(\epsilon_{\mathbf{k}})}{\epsilon_{\mathbf{k}}(\omega^2 - 4\epsilon_{\mathbf{k}}^2)}\delta_+(\omega) \tag{A12}$$

$$M_{\mathbf{k}}(\omega) = \frac{\mathrm{i}m_{\mathbf{k}}(0^-)}{\omega}, \tag{A13}$$

and finally to eliminate them using the resummation Eq. (A9), yielding a closed system of equations on $\delta_\pm$:

$$M\begin{pmatrix}\delta-\delta^*\\ \delta+\delta^*\end{pmatrix}=-\mathrm{i}\begin{pmatrix}S_-\\ S_+\end{pmatrix}. \tag{A14}$$

The fluctuation matrix M is introduced below Eq. (7) of the main text, and the sums encoding the initial conditions on Δ are given by

$$S_+=\int\frac{\mathrm{d}^3\mathbf{k}}{(2\pi)^3}\left[\frac{\omega\xi_\mathbf{k}\alpha_\mathbf{k}^+(0^-)+2\xi_\mathbf{k}\epsilon_\mathbf{k}\alpha_\mathbf{k}^-(0^-)}{\epsilon_\mathbf{k}(\omega^2-4\epsilon_\mathbf{k}^2)}+\frac{\Delta_i}{\epsilon_\mathbf{k}}\frac{m_\mathbf{k}(0^-)}{\omega}\right]+\frac{\delta\Delta_0+\delta\Delta_0^*}{g_i\omega} \tag{A15}$$

$$S_-=\int\frac{\mathrm{d}^3\mathbf{k}}{(2\pi)^3}\frac{\omega\alpha_\mathbf{k}^-(0^-)+2\epsilon_\mathbf{k}\alpha_\mathbf{k}^+(0^-)}{\omega^2-4\epsilon_\mathbf{k}^2}+\frac{\delta\Delta_0-\delta\Delta_0^*}{g_i\omega}. \tag{A16}$$

Inverting Eq. (A14) and switching back to the time domain [using the inverse Laplace transformation $f(t)=-\frac{1}{2\pi}\int_{+\infty+\mathrm{i}\eta}^{-\infty+\mathrm{i}\eta}\mathrm{d}z\mathrm{e}^{-\mathrm{i}zt}F(z)$] yields, for the time-evolution of Δ,

$$\begin{pmatrix}\delta\Delta(t)-\delta\Delta^*(t)\\ \delta\Delta(t)+\delta\Delta^*(t)\end{pmatrix}=-\int_{+\infty+\mathrm{i}\eta}^{-\infty+\mathrm{i}\eta}\frac{\mathrm{d}z}{2\mathrm{i}\pi}\mathrm{e}^{-\mathrm{i}zt}M^{-1}\begin{pmatrix}S_-\\ S_+\end{pmatrix}. \tag{A17}$$

We now input the initial condition corresponding to the interaction quench, that is [as explained above Eq. (3) of the main text], $\alpha_\mathbf{k}^\pm=m_\mathbf{k}=0$, and $\delta\Delta_0=\epsilon g_i/\Delta_i$, which converts into $S_-=0$ and $S_+=2\epsilon/\omega\Delta_i$. Finally, we derive Eq. (6) of the main text by closing the integration contour in Eq. (A17) around the branch cuts of M (see Fig. 1 in Ref. [7]), and by remarking that the modulus-modulus response function [Eq. (7)] is related to M by $f(z)=-(M^{-1})_{22}/\Delta_i$.

Appendix B: Adiabatic derivative of Δ. To form the ratio $(\Delta_\infty-\Delta_i)/(\Delta_f-\Delta_i)$ plotted in Fig. 1 we must evaluate the adiabatic derivative

$$\frac{\mathrm{d}(1/k_Fa)}{\mathrm{d}\Delta}=\frac{1/k_Fa_f-1/k_Fa_i}{\Delta_f-\Delta_i}. \tag{B1}$$

We do so by deriving the gap equation

$$\frac{1}{g}=-\int\frac{d^3k}{(2\pi)^3}\frac{1-2F(\epsilon_\mathbf{k})}{2\epsilon_\mathbf{k}} \tag{B2}$$

with respect to Δ at fixed density $\rho=k_F^3/3\pi^2$ and temperature T. This yields

$$\left.\frac{\mathrm{d}(1/k_Fa)}{\mathrm{d}\Delta}\right|_{\rho,T}=\frac{2\pi}{mk_F\Delta^2}\left[I_0-J_0-\frac{\mathrm{d}\mu}{\mathrm{d}\Delta}(I_1-J_1)\right], \tag{B3}$$

where we have introduced the integrals

$$I_n=\int\frac{\mathrm{d}^3k}{(2\pi)^3}\frac{\Delta^{3-n}\xi_\mathbf{k}^n}{\epsilon_\mathbf{k}^3}[1-2F(\epsilon_\mathbf{k})], \tag{B4}$$

$$J_n=\int\frac{\mathrm{d}^3k}{(2\pi)^3}\frac{\Delta^{3-n}\xi_\mathbf{k}^n}{\epsilon_\mathbf{k}^2}[-2F'(\epsilon_\mathbf{k})]. \tag{B5}$$

The derivative of the chemical potential is evaluated by deriving the number equation $\rho=\int\frac{\mathrm{d}^3k}{(2\pi)^3}[1-\xi_\mathbf{k}F(\epsilon_\mathbf{k})/\epsilon_\mathbf{k}]$:

$$\left.\frac{\mathrm{d}\mu}{\mathrm{d}\Delta}\right|_{\rho,T}=\frac{-I_1+J_1}{I_0+J_2}. \tag{B6}$$

The variation of Δ during the quench is given by (8) of the main text, which we rewrite as

$$\frac{\Delta_\infty-\Delta_i}{1/k_Fa_f-1/k_Fa_i}=-\frac{m\Delta_i^2k_F}{4\pi}f(0), \tag{B7}$$

where $f(0)=-2I_0/(I_0^2+I_1^2)$ in terms of the integrals introduced in Eq. (B4). Combining this with the adiabatic derivative Eq. (B3), we obtain

$$\begin{aligned}\frac{\Delta_\infty-\Delta_i}{\Delta_f-\Delta_i}&=\frac{\Delta_\infty-\Delta_i}{1/k_Fa_f-1/k_Fa_i}\frac{\mathrm{d}(1/k_Fa)}{\mathrm{d}\Delta}\\&=\frac{I_0}{I_0^2+I_1^2}\left[I_0-J_0+\frac{(I_1-J_1)^2}{I_0+J_2}\right]\\&\underset{1/k_Fa_i\to-\infty}{\to}1-\frac{J_0}{I_0}.\end{aligned} \tag{B8}$$

[1] L. Pitaevskii and S. Stringari, *Bose–Einstein Condensation and Superfluidity* (Oxford University, Oxford, 2016).
[2] R. Haussmann, M. Punk, and W. Zwerger, Phys. Rev. A **80**, 063612 (2009).
[3] R. G. Scott, F. Dalfovo, L. P. Pitaevskii, and S. Stringari, Phys. Rev. A **86**, 053604 (2012).
[4] A. F. Volkov and S. M. Kogan, Zh. Eksp. Teor. Fiz. **65**, 2038 (1973) [Sov. Phys. JETP **38**, 1018 (1974)].
[5] D. Pekker and C. Varma, Annu. Rev. Condens. Matter Phys. **6**, 269 (2015).
[6] A. Schmid, Phys. Kondens. Mater. **8**, 129 (1968).
[7] V. Gurarie, Phys. Rev. Lett. **103**, 075301 (2009).
[8] E. A. Yuzbashyan, M. Dzero, V. Gurarie, and M. S. Foster, Phys. Rev. A **91**, 033628 (2015).
[9] V. A. Andrianov and V. N. Popov, Theor. Math. Phys. **28**, 829 (1976).
[10] H. Kurkjian, S. N. Klimin, J. Tempere, and Y. Castin, Phys. Rev. Lett. **122**, 093403 (2019).
[11] A. Behrle, T. Harrison, J. Kombe, K. Gao, M. Link, J.-S. Bernier, C. Kollath, and M. Köhl, Nat. Phys. **14**, 781 (2018).
[12] P. Dyke, S. Musolino, H. Kurkjian, D. J. M. Ahmed-Braun, A. Pennings, I. Herrera, S. Hoinka, S. J. J. M. F. Kokkelmans, V. E. Colussi, and C. J. Vale, arXiv:2310.03452 [Phys. Rev. Lett. (to be published)].
[13] R. Matsunaga, Y. I. Hamada, K. Makise, Y. Uzawa, H. Terai, Z. Wang, and R. Shimano, Phys. Rev. Lett. **111**, 057002 (2013).
[14] R. J. Lewis-Swan, D. Barberena, J. R. K. Cline, D. J. Young, J. K. Thompson, and A. M. Rey, Phys. Rev. Lett. **126**, 173601 (2021).
[15] D. J. Young, A. Chu, E. Y. Song, D. Barberena, D. Wellnitz, Z. Niu, V. M. Schäfer, R. J. Lewis-Swan, A. M. Rey, and J. K. Thompson, Nature (London) **625**, 679 (2024).

[16] *The BCS-BEC Crossover and the Unitary Fermi Gas*, edited by W. Zwerger (Springer, Berlin, 2012).
[17] J.-P. Blaizot and G. Ripka, *Quantum Theory of Finite Systems* (MIT, Cambridge, 1985).
[18] J. R. Taylor, *Scattering Theory: The Quantum Theory of Non-relativistic Collisions* (Courier Corporation, North Chelmsford, 2006).
[19] Y. Castin, in *Ultra-Cold Fermi Gases*, edited by M. Inguscio, W.Ketterle, and C. Salomon (Società Italiana di Fisica, Bologna, 2007).
[20] F. Werner and Y. Castin, Phys. Rev. A **86**, 013626 (2012).
[21] R. Qi, Z. Shi, and H. Zhai, Phys. Rev. Lett. **126**, 240401 (2021).
[22] S. Tan, Ann. Phys. **323**, 2952 (2008).
[23] S. Tan, Ann. Phys. **323**, 2971 (2008).
[24] S. Tan, Ann. Phys. **323**, 2987 (2008).
[25] E. Braaten, D. Kang, and L. Platter, Phys. Rev. A **78**, 053606 (2008).
[26] Y. Castin and H. Kurkjian, C. R.. Phys. **21**, 253 (2020).
[27] S. N. Klimin, J. Tempere, and H. Kurkjian, Phys. Rev. A **100**, 063634 (2019).
[28] See Supplemental Material at http://link.aps.org/supplemental/10.1103/PhysRevA.109.L041302 for appendix C explaining how to calculate analytically the coefficients of amplitude oscillations in limit $T \to T_c$, and appendix D providing technical details useful for the numerical evaluation of the modulus response function.
[29] P. Dyke, A. Hogan, I. Herrera, C. C. N. Kuhn, S. Hoinka, and C. J. Vale, Phys. Rev. Lett. **127**, 100405 (2021).
[30] P. Pieri, L. Pisani, and G. C. Strinati, Phys. Rev. B **70**, 094508 (2004).
[31] H. Hu, X.-J. Liu, P. D. Drummond, and H. Dong, Phys. Rev. Lett. **104**, 240407 (2010).
[32] H. Kurkjian and J. Tempere, New J. Phys. **19**, 113045 (2017).